Towards a Topology-Shape-Metrics Framework for Ortho-Radial Drawings*

Lukas Barth†[1], Benjamin Niedermann[2], Ignaz Rutter[3], and Matthias Wolf[4]

1 **Karlsruhe Institute of Technology, Karlsruhe, Germany**
`lukas.barth@kit.edu`
2 **University of Bonn, Bonn, Germany**
`niedermann@uni-bonn.de`
3 **TU Eindhoven, Eindhoven, The Netherlands**
`i.rutter@tue.nl`
4 **Karlsruhe Institute of Technology, Karlsruhe, Germany**
`matthias.wolf@kit.edu`

Abstract

Ortho-Radial drawings are a generalization of orthogonal drawings to grids that are formed by concentric circles and straight-line spokes emanating from the circles' center. Such drawings have applications in schematic graph layouts, e.g., for metro maps and destination maps.

A plane graph is a planar graph with a fixed planar embedding. We give a combinatorial characterization of the plane graphs that admit a planar ortho-radial drawing without bends. Previously, such a characterization was only known for paths, cycles, and theta graphs [12], and in the special case of rectangular drawings for cubic graphs [11], where the contour of each face is required to be a rectangle.

The characterization is expressed in terms of an *ortho-radial representation* that, similar to Tamassia's *orthogonal representations* for orthogonal drawings describes such a drawing combinatorially in terms of angles around vertices and bends on the edges. In this sense our characterization can be seen as a first step towards generalizing the Topology-Shape-Metrics framework of Tamassia to ortho-radial drawings.

1998 ACM Subject Classification G.2.2 Graph Theory

Keywords and phrases Graph Drawing, Ortho-Radial Drawings, Combinatorial Characterization, Bend Minimization, Topology-Shape-Metrics

Digital Object Identifier 10.4230/LIPIcs.SoCG.2017.14

1 Introduction

Grid drawings of graphs map vertices to grid points, and edges to internally disjoint curves on the grid lines connecting their endpoints. The appropriate choice of the underlying grid is decisive for the quality and properties of the drawing. *Orthogonal grids*, where the grid lines are horizontal and vertical lines, are popular and widely used in graph drawing. Their strength lies in their simple structure, their high angular resolution, and the limited number of directions. Graphs admitting orthogonal grid drawings must be *4-planar*, i.e., they must be planar and have maximum degree 4. On such grids a single edge consists of a sequence

* A full version of the paper is available at `https://arxiv.org/abs/1703.06040`.
† Lukas Barth's research was partially supported by DFG Research Training Group 2153

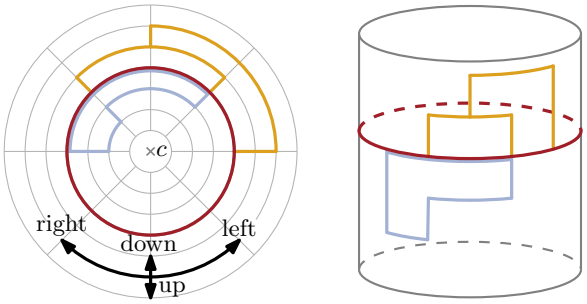

(a) Ortho-Radial Grid. **(b)** Cylinder.

Figure 1 An ortho-radial drawing of a graph on a grid **(a)** and its equivalent interpretation as an orthogonal drawing on a cylinder **(b)**.

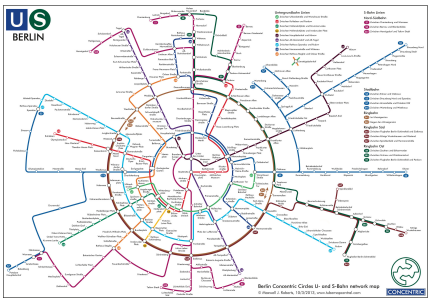

Figure 2 Metro map of Berlin using an ortho-radial layout. Image copyright by Maxwell J. Roberts.

of horizontal and vertical grid segments. A transition between a horizontal and a vertical segment on an edge is called a *bend*. A typical optimization goal is to minimize the number of bends in the drawing, either in total or by the maximum number of bends per edge.

The popularity and usefulness of orthogonal drawing have their foundations in the seminal work of Tamassia [15] who showed that for *plane graphs*, i.e., planar graphs with a fixed embedding, a bend-minimal planar orthogonal drawing can be computed efficiently. More generally, Tamassia [15] established the so-called Topology-Shape-Metrics framework, abbreviated as TSM in the following, for computing orthogonal drawings of 4-planar graphs.

The goal of this work is to provide a similar framework for *ortho-radial drawings*, which are based on ortho-radial grids rather than orthogonal grids. Such drawings have applications in schematic graph layouts, e.g., for metro maps and destination maps; see Fig. 2 for an example. An *ortho-radial grid* is formed by M concentric circles and N spokes, where $M, N \in \mathbb{N}$. More precisely, the radii of the concentric circles are integers, and the N spokes emanate from the center $c = (0, 0)$ of the circles such that they have uniform angular resolution; see Fig. 1. We note that c does not belong to the grid. Again vertices are positioned at grid points and edges are drawn as internally disjoint chains of (1) segments of spokes and (2) arcs of concentric circles. As before, a *bend* is a transition between a spoke segment and an arc segment. We observe that ortho-radial drawings can also be thought of as orthogonal drawings on a cylinder; see Fig. 1. Edge segments that are originally drawn on spokes are parallel to the axis of the cylinder, whereas segments that are originally drawn as arcs are drawn on circles orthogonal to the axis of the cylinder.

It is not hard to see that every orthogonal drawing can be transformed into an ortho-radial drawing with the same number of bends. The converse is, however, not true. It is readily seen that for example a triangle, which requires at least one bend in an orthogonal drawing, admits an ortho-radial drawing without bends, namely in the form of a circle centered at the origin. In fact, by suitably nesting triangles, one can construct graphs that have an ortho-radial drawing without bends but require a linear number of bends in any orthogonal drawing.

Related Work. The case of planar orthogonal drawings is well-researched and there is a plethora of results known; see [9] for a survey. Here, we mention only the most recent results and those which are most strongly related to the problem we consider. A k-embedding is an orthogonal planar drawing such that each edge has at most k bends. It is known that, with

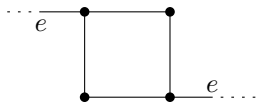

Figure 3 In this drawing, the angles around vertices sum up to 360°, and also the sum of angles for each face is as expected for an ortho-radial drawing. However, the graph does not have an ortho-radial drawing without bends.

the single exception of the octahedron graph, every planar graph has a 2-embedding [2] and that deciding the existence of a 0-embedding is $\mathcal{NP}$-complete [10]. The latter in particular implies that the problem of computing a planar orthogonal drawing with the minimum number of bends is $\mathcal{NP}$-hard. In contrast, the existence of a 1-embedding can be tested efficiently [3]; this has subsequently been generalized to a version that forces up to k edges to have no bends in FPT time w.r.t. k [4], and to an optimization version that optimizes the number of bends beyond the first one on each edge [5]. Moreover, for series-parallel graphs and graphs with maximum degree 3 an orthogonal planar drawing with the minimum number of bends can be computed efficiently [8].

The $\mathcal{NP}$-hardness of the bend minimization problem has also inspired the study of bend minimization for planar graphs with a fixed embedding. In his fundamental work Tamassia [15] showed that for plane graphs, i.e., planar graphs with a fixed planar embedding, bend-minimal planar orthogonal drawings can be computed in polynomial time. The running time has subsequently been improved to $O(n^{1.5})$ [6]. Key to these results is the existence of a combinatorial description of planar orthogonal drawings of a plane graph in terms of the angles surrounding each vertex and the order and directions of bends on the edges but neglecting any kind of geometric information such as coordinates and edge lengths. In particular, this allows to efficiently compute bend-minimal orthogonal drawings of plane graphs by mapping the purely combinatorial problem of determining an orthogonal representation with the minimum number of bends to a flow problem.

In addition, there is a number of works that seek to characterize the plane graphs that can be drawn without bends. In this case an orthogonal representation essentially only describes the angles around the vertices. Rahman, Nishizeki and Naznin [14] characterize the plane graphs with maximum degree 3 that admit such a drawing and Rahman, Nakano and Nishizeki [13] characterize the plane graphs that admit a rectangular drawing where in addition the contour of each face is a rectangle.

In the case of ortho-radial drawings much less is known. A natural generalization of the properties of an orthogonal representation to the ortho-radial case, where the angles around the vertices and inside the faces are constrained, has turned out not be sufficient for drawability; see Fig. 3. So far characterizations of bend-free ortho-radial drawing have only been achieved for paths, cycles, and theta graphs [12]. For the special case of rectangular ortho-radial drawings, i.e., every internal face is bounded by a rectangle, a characterization is known for cubic graphs [11].

Contribution and Outline. Since deciding whether a 4-planar graph can be orthogonally drawn in the plane without any bends is $\mathcal{NP}$-complete [10], it is not surprising that also ortho-radial bend minimization is $\mathcal{NP}$-hard; the proof is in the full version [1] of this paper.

▶ **Theorem 1.1.** *Deciding whether a 4-planar graph has a planar ortho-radial drawing without any bends is $\mathcal{NP}$-complete.*

As our main result we introduce a generalization of an orthogonal representation, which we call *ortho-radial representation*, that characterizes the *4-plane graphs*, i.e., 4-planar graphs with a fixed combinatorial embedding, having bend-free ortho-radial drawings; see Theorem 3.5.

This significantly generalizes the corresponding results for paths, cycles, theta graphs [12], and cubic graphs [11]. Further, this characterization can be seen as a step towards an extension of the TSM framework for computing ortho-radial drawings that may have bends. Namely, once the angles around vertices and the order and directions of bends along each edge of a graph G have been fixed, we can replace each bend by a vertex to obtain a graph G'. The directions of bends and the angles at the vertices of G define a unique ortho-radial representation of G', which is valid if and only if G admits a drawing with the specified angles and bends. Thus, ortho-radial drawings can indeed be described by angles around vertices and orders and directions of bends on edges. Our main result therefore implies that ortho-radial drawings can be computed by a TSM framework, i.e., by fixing a combinatorial embedding in a first "Topology" step, determining a description of the drawing in terms of angles and bends in a second "Shape" step, and computing edge lengths and vertex coordinates in a final "Metrics" step.

In the following, we disregard the "Topology" step and assume that our input consists of a 4-planar graph with a fixed *combinatorial embedding*, i.e., the order of the incident edges around each vertex is fixed and additionally, one outer face and one central face are specified; the latter shall contain the center of the drawing. We present our definition of an ortho-radial representation in Section 3. After introducing some basic tools based on this representation in Section 4, we first present in Section 5 a characterization for rectangular graphs, whose ortho-radial representation is such that internal faces have exactly four 90° angles, while all other incident angles are 180°; i.e., they have to be drawn as rectangles.

The algorithm we use as a proof of drawability corresponds to the "Metrics" step of an ortho-radial TSM framework. The characterization corresponds to the output of the "Shape" step. Based on the special case of rectangular 4-planar graphs, we then present the characterization and the "Metrics" step for general 4-planar graphs in Section 6. Due to space constraints, some proofs are omitted or only sketched; full proofs can be found in the full version of this paper [1].

2 Ortho-Radial Drawings

In this section we introduce basic definitions and conventions on ortho-radial drawings that we use throughout this paper. To that end, we first introduce some basic definitions.

We assume that paths cannot contain vertices multiple times but cycles can, i.e., all paths are simple. We always consider non-selfcrossing cycles as directed clockwise, so that their interior is locally to the right of the cycle. A cycle is part of its interior and its exterior.

For a path P and vertices u and v on P, we denote the subpath of P from u to v (including these vertices) by $P[u, v]$. We may also specify the first and last edge instead and write, e.g., $P[e, e']$ for edges e and e' on P. We denote the concatenation of two paths P and Q by $P + Q$. For a path $P = v_1 \dots v_k$, we define its reverse $\overline{P} = v_k \dots v_1$. For a cycle C that contains any edge at most once (e.g. if C is simple), we extend the notion of subpaths as follows. For two edges e and e' on C, the subpath $C[e, e']$ is the unique path on C that starts with e and ends with e'. If the start vertex v of e identifies e uniquely, i.e., C contains v exactly once, we may write $C[v, e']$ to describe the path on C from v to e'. Analogously, we may identify e' with its endpoint if this is unambiguous.

We are now ready to introduce concepts of ortho-radial drawings. Consider a 4-planar graph $G = (V, E)$ with fixed embedding. We refer to the directed edge from u to v by uv. Let Δ be an ortho-radial drawing of G, and recall that we do not allow bends on edges. In Δ a directed edge e is either drawn clockwise, counter-clockwise, towards the center or away from the center; see Fig. 1. Using the metaphor of drawing G on a cylinder, we say that e points *right*, *left*, *down* or *up*, respectively. Edges pointing left or right are *horizontal* edges and edges pointing up or down are *vertical* edges.

There are two fundamentally different ways of drawing a simple cycle C. The center of the grid may lie in the interior or the exterior of C. In the former case C is *essential* and in the latter case it is *non-essential*. In Fig. 1 the red cycle is essential and the blue cycle is non-essential.

We further observe that Δ has two special faces: One unbounded face, called the *outer face*, and the *central face* containing the center of the drawing. These two faces are equal if and only if Δ contains no essential cycles. All other faces of G are called *regular*. Ortho-radial drawings without essential cycles are equivalent to orthogonal drawings [12]. That is, any such ortho-radial drawing can be transformed to an orthogonal drawing of the same graph with the same outer face and vice versa.

We represent a face as a cycle f in which the interior of the face lies locally to the right of f. Note that f may not be simple since cut vertices may appear multiple times on f. But no directed edge is used twice by f. Therefore, the notation of subpaths of cycles applies to faces. Note furthermore that the cycle bounding the outer face of a graph is directed counter-clockwise, whereas all other faces are bounded by cycles directed clockwise.

A face f in Δ is a *rectangle* if and only if its boundary does not make any left turns. That is, if f is a regular face, there are exactly 4 right turns, and if f is the central or the outer face, there are no turns at all. Note that by this definition f cannot be a rectangle if it is both the outer and the central face.

3 Ortho-Radial Representations

In this section, we define ortho-radial representations. These are a tool to describe the ortho-radial drawing of a graph without fixing any edge lengths. As mentioned in the introduction, they are an analogon to orthogonal representations in the TSM framework.

We observe all directions of all edges being fixed once the direction of one edge and all angles around vertices are fixed. For two edges uv and vw that enclose the angle $\alpha \in \{90°, 180°, 270°, 360°\}$ at v (such that the angle measured lies locally to the right of uvw), we define the rotation $\mathrm{rot}(uvw) = 2 - \alpha/90°$. We note that the rotation is 1 if there is a right turn at v, 0 if uvw is straight, and -1 if a left turn occurs at v. If $u = w$, it is $\mathrm{rot}(uvw) = -2$.

We define the rotation of a path $P = v_1 \dots v_k$ as the sum of the rotations at its internal vertices, i.e., $\mathrm{rot}(P) = \sum_{i=2}^{k-1} \mathrm{rot}(v_{i-1}v_iv_{i+1})$. Similarly, for a cycle $C = v_1 \dots v_k v_1$, its rotation is the sum of the rotations at all its vertices, i.e., $\mathrm{rot}(C) = \sum_{i=1}^{k} \mathrm{rot}(v_{i-1}v_iv_{i+1})$, where we define $v_0 = v_k$ and $v_{k+1} = v_1$.

When splitting a path at an edge, the sum of the rotations of the two parts is equal to the rotation of the whole path.

▶ **Observation 3.1.** *Let P be a simple path with start vertex s and end vertex t. For all edges e on P it holds that* $\mathrm{rot}(P) = \mathrm{rot}(P[s, e]) + \mathrm{rot}(P[e, t])$.

Furthermore, reversing a path changes all left turns to right turns and vice versa. Hence, the sign of the rotation is flipped.

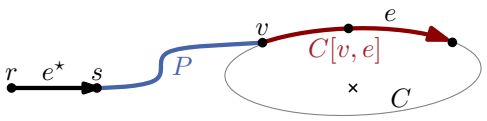

Figure 4 The labeling of e induced by P is $\ell_C^P(e) = \mathrm{rot}(e^\star + P + C[v,e])$.

▶ **Observation 3.2.** *For any path P it is* $\mathrm{rot}(\overline{P}) = -\mathrm{rot}(P)$.

The next observation analyzes *detours*; an illustration is found in [1].

▶ **Observation 3.3.** *Let P be a path from v to w and xy an edge not on P such that x is an internal vertex of P. It is* $\mathrm{rot}\,(P[v,x] + xy) + \mathrm{rot}\,(yx + P[x,w]) = \mathrm{rot}\,(P) + c$, *where $c = -2$ if xy lies locally to the right of P and $c = +2$ if xy lies locally to the left of P.*

An *ortho-radial representation* of a 4-planar graph G consists of a list $H(f)$ of pairs (e, a) for each face f, where e is an edge on f, and $a \in \{90°, 180°, 270°, 360°\}$. Further, the outer face and the central face are fixed and one *reference edge* $e^\star$ in the outer face is given, with $e^\star$ oriented such that the outer face is locally to its left. By convention the reference edge is always drawn such that it points right. We interpret the fields of a pair in $H(f)$ as follows. e denotes the edge on f directed such that f lies to the right of e. The field a represents the angle inside f from e to the following edge in degrees. Using this information we define the *rotation* of such a pair $t = (e, a)$ as $\mathrm{rot}(t) = (180° - a)/90°$.

Not every ortho-radial representation also yields an ortho-radial drawing of a graph. In order to characterize valid ortho-radial representations, we introduce *labelings* of essential cycles. These labelings prove to be a valuable tool to ensure that all the essential cycles of the graph can be drawn in such a way that they are compatible with each other.

Let G be an embedded 4-planar graph and let $e^\star = rs$ be the reference edge of G. Further, let C be a simple, essential cycle in G, and let P be a path from s to a vertex v on C. The *labeling* ℓ_C^P of C induced by P is defined for each edge e on C by $\ell_C^P(e) = \mathrm{rot}(e^\star + P + C[v,e])$; see Fig. 4 for an illustration. We are mostly interested in labelings that are induced by paths starting at s and intersecting C only at their endpoints. We call such paths *elementary paths*.

We now introduce properties characterizing bend-free ortho-radial drawings, as we prove in Theorem 3.5.

▶ **Definition 3.4.** An ortho-radial representation is *valid* if the following conditions hold:

1. The angle sum of all edges around each vertex given by the a-fields is 360.
2. For each face f, it is

$$\mathrm{rot}(f) = \begin{cases} 4, & f \text{ is a regular face} \\ 0, & f \text{ is the outer or the central face but not both} \\ -4, & f \text{ is both the outer and the central face} \end{cases}$$

3. For each simple, essential cycle C in G, there is a labeling ℓ_C^P of C induced by an elementary path P such that either $\ell_C^P(e) = 0$ for all edges e of C, or there are edges e_+ and e_- on C such that $\ell_C^P(e_+) > 0$ and $\ell_C^P(e_-) < 0$.

The first two conditions ensure that the angle-sums at vertices and inside the faces are correct. Since the labels of neighboring edges differ by at most 1, the last condition ensures that on each essential cycle with not only horizontal edges there are edges with labels 1 and -1, i.e., edges pointing up and down. This reflects the characterization for cycles [12].

Intuitively, basing all labels on the reference edge guarantees that all cycles in the graph can be drawn together consistently.

For an essential cycle C not satisfying the last condition there are two possibilities. Either all labels of edges on C are non-negative and at least one label is positive, or all are non-positive and at least one is negative. In the former case C is called *decreasing* and in the latter case it is *increasing*. We call both *monotone* cycles. Cycles with only the label 0 are not monotone.

We show that a graph with a given ortho-radial representation can be drawn if and only if the representation is valid, which yields our main result.

▶ **Theorem 3.5.** *A 4-plane graph admits a bend-free orthogonal drawing if and only if it admits a valid ortho-radial representation.*

While we defer the proof that the conditions for valid ortho-radial representations are sufficient for the existence of a drawing to Section 6.2, the necessity of the conditions is easier to see.

▶ **Theorem 3.6.** *For any ortho-radial drawing Δ of a 4-planar graph G there is a valid ortho-radial representation of G.*

Proof Sketch. We note that any drawing Δ fixes an ortho-radial representation up to the choice of the reference edge. Let Γ be such an ortho-radial representation where we pick an edge $e^\star$ on the outer face as the reference edge such that $e^\star$ points to the right and lies on the outermost circle that is used by Δ. By [12] the representation Γ satisfies Conditions 1 and 2 of Definition 3.4. To prove that Γ also satisfies Condition 3, i.e., Γ does not contain any monotone cycles, we reduce the general case to the more restricted one where all faces are rectangles. To that end we geometrically augment Δ to Δ' such that all faces are rectangles. Given an essential cycle C in Δ' we iteratively construct a path P from the topmost point of C in Δ' to $e^\star$ such that each edge on P goes either up or left. For this Δ' needs to be rectangular. We show that the reversed path $\overline{P}$ induces a labeling of C that is 0 on each edge or has positive and negative labels. ◀

In the next section, we introduce further tools based on labelings. Subsequently, in Section 5 we prove Theorem 3.5 for rectangular graphs. In Section 6, we generalize the result to 4-planar graphs.

4 Properties of Labelings

In this section we study the properties of labelings in more detail to derive useful tools for proving Theorem 3.5. Throughout this section, G is a 4-planar graph with ortho-radial representation Γ that satisfies Conditions 1 and 2 of Definition 3.4. Further let $e^\star$ be a reference edge. From Condition 2 we obtain that the rotation of all essential cycles is 0.

▶ **Observation 4.1.** *For any simple essential cycle C of G it is* $\mathrm{rot}(C) = 0$.

Together with the reference edge, an ortho-radial representation fixes the direction of all edges. For the direction of an edge e, we consider a path P from the reference edge to e including both edges. Different such paths may have different rotations but we observe that these rotations differ by a multiple of 4. An edge e is directed *right*, *down*, *left*, or *up*, if $\mathrm{rot}(P)$ is congruent to 0, 1, 2, or 3 modulo 4, respectively. Note that by this definition the reference edge always points to the right. Because the rotation of essential cycles is 0 by Observation 4.1, for two edges on an essential cycle we observe the following.

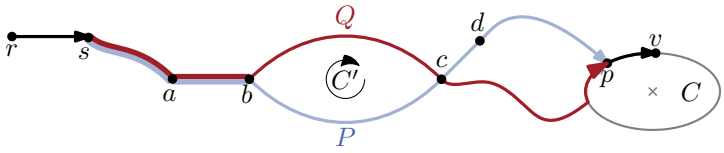

Figure 5 Two paths P and Q from s to p. The cycle C' is formed by $Q[b,c]$ and $\overline{P}[c,b]$.

▶ **Observation 4.2.** *For any path P and for any two edges e and e' on a simple, essential cycle C, it holds that* $\mathrm{rot}(C[e,e']) = \ell_C^P(e') - \ell_C^P(e)$.

We now show that two elementary paths to the same essential cycle C induce identical labelings of C. Two paths P and Q from $e^\star$ to vertices on C are *equivalent* ($P \equiv_C Q$) if the corresponding labelings agree on all edges of C, i.e., $\ell_C^P(e) = \ell_C^Q(e)$ for every edge e of C.

▶ **Lemma 4.3.** *Let C be an essential cycle in G and let $e^\star = rs$. If P and Q are paths from s to vertices on C such that P and Q lie in the exterior of C, they are equivalent.*

Proof Sketch. From the definition of labelings it is not hard to see that two paths P and Q are equivalent if there exists an edge e on C with $\ell_C^P(e) = \ell_C^Q(e)$.

We prove the equivalence of P and Q by showing that such an edge e exists. To that end assume that one of the paths, say Q, is elementary. Let p and q be the endpoints of P and Q, respectively. Let v be the vertex following p on C when C is directed such that the central face lies in its interior. We define $Q' = Q + C[q,p]$. It is easy to verify that both P and Q' are paths that lie in the exterior of C. We show that

$$\ell_C^P(pv) = \mathrm{rot}(e^\star + P + pv) = \mathrm{rot}(e^\star + Q' + pv) = \ell_C^Q(pv). \tag{1}$$

Hence, the edge pv is the desired edge e. So far we have assumed that Q is elementary. If neither P nor Q are elementary, choose any elementary path R to a vertex on C. The argument above shows that $P \equiv_C R$ and $R \equiv_C Q$, and thus $P \equiv_C Q$.

To show Equation 1 we do an induction over the number k of directed edges on Q that do not lie on P. Without loss of generality we assume that Q also ends at p; otherwise we extend Q to $Q + C[q,p]$. If $k = 0$, P contains Q completely and the claim follows immediately.

If $k > 0$, there is a first edge ab on Q such that the following edge does not lie on P. Let c be the first vertex on Q after b that lies on P and let d be the vertex on $P + pv$ that follows c immediately. Fig. 5 illustrates the situation. Consider the cycle $C' = Q[b,c] + \overline{P}[c,b]$. For both cases, namely that C' is essential and C' is non-essential, we argue that $\mathrm{rot}(ab + P[b,c] + cd) = \mathrm{rot}(ab + Q[b,c] + cd)$.

In both cases it then follows from $P[s,b] = Q[s,b]$ that $\mathrm{rot}(rs + P[s,c] + cd) = \mathrm{rot}(rs + Q[s,c] + cd)$. For $P' = Q[s,c] + P[c,p]$ it therefore holds that $\mathrm{rot}(rs + P + pv) = \mathrm{rot}(rs + P' + pv)$. As P' includes the part of Q between b and c it misses fewer edges from Q than P does. Hence, the inductive hypothesis implies $\mathrm{rot}(rs + Q + pv) = \mathrm{rot}(rs + P' + pv)$, and thus $\mathrm{rot}(rs + Q + pv) = \mathrm{rot}(rs + P + pv)$. ◀

In the remainder of this section all labelings are induced by elementary paths. By Lemma 4.3, the labelings are independent of the choice of the elementary path. Hence, we drop the superscript P and write $\ell_C(e)$ for the labeling of an edge e on an essential cycle C.

If an edge e lies on two simple, essential cycles C_1 and C_2, the labels $\ell_{C_1}(e)$ and $\ell_{C_2}(e)$ may not be equal in general. In Fig. 6a the labels of the edge e are different for C_1 and C_2 respectively, but e' has label 0 on both cycles. Note that e' is incident to the central face of

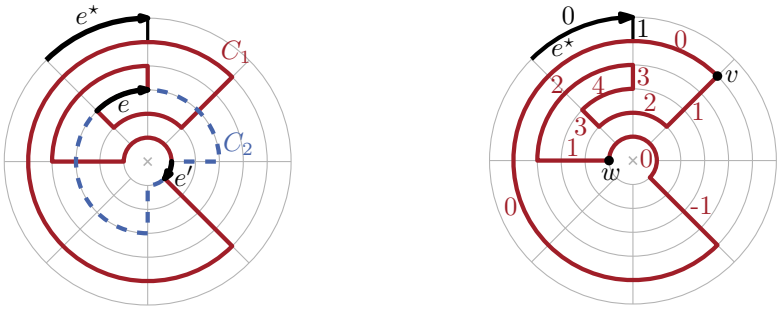

(a) (b)

Figure 6 (a) Two cycles C_1 and C_2 may have both common edges with different labels ($\ell_{C_1}(e) = 4 \neq 0 = \ell_{C_2}(e)$) and ones with equal labels ($\ell_{C_1}(e') = \ell_{C_2}(e') = 0$). (b) All labels of $C_1[v, w]$ are positive, implying that C_1 goes down. Note that not all edges of $C_1[v, w]$ point downwards.

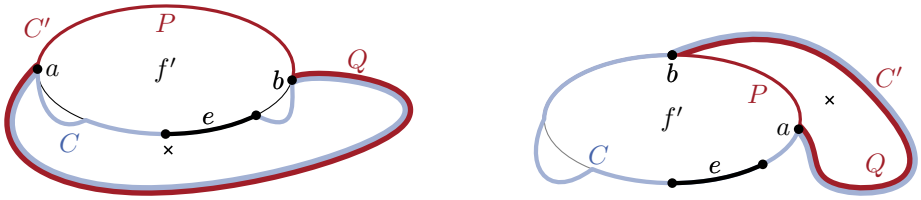

(a) The cycle bounding the outer face is C'. **(b)** The cycle bounding the central face is C'.

Figure 7 The edge e cannot lie on both the outer and the central face, which is marked by a cross. (a) e does not lie on the outer face, and hence the cycle bounding this face is defined as C'. (b) C' is the cycle bounding the central face. In both cases C' can be subdivided in two paths P and Q on C and f', respectively. Here, these paths are separated by the vertices a and b.

$C_1 + C_2$. One can show that this is a sufficient condition for the equality of the labels; see the full version [1] for a proof.

▶ **Lemma 4.4.** *Let C_1 and C_2 be two essential cycles and let $H = C_1 + C_2$ be the subgraph of G formed by these two cycles. Let v be a common vertex of C_1 and C_2 on the central face of H and consider the edge vw on C_1. Denote the vertices before v on C_1 and C_2 by u_1 and u_2, respectively. Then $\ell_{C_1}(u_1v) + \mathrm{rot}(u_1vw) = \ell_{C_2}(u_2v) + \mathrm{rot}(u_2vw)$.*

Further, if vw belongs to both C_1 and C_2, the labels of e are equal, i.e., $\ell_{C_1}(vw) = \ell_{C_2}(vw)$.

For the correctness proof in Section 6, a crucial insight is that for cycles using an edge which is part of a face, we can find an alternative cycle without this edge in a way that preserves labels on the common subpath, which we show in the next lemma; see Fig. 7 for an illustration.

▶ **Lemma 4.5.** *If an edge e belongs to both a simple essential cycle C and a regular face f' with $C \neq f'$, then there is a simple essential cycle C' not containing e such that C' can be decomposed into two paths P and Q, where P or $\overline{P}$ lies on f' and $Q = C \cap C'$.*

Applying this lemma on an edge e, we construct an essential cycle C' without e from an essential cycle C including e. Also, C and C' have a common path P lying on the central face of $C + f'$. Thus, Lemma 4.4 implies labelings of C and C' being equal on P.

▶ **Corollary 4.6.** *For essential cycles C, C' and the path $P = C \cap C'$ from Lemma 4.5, it is $\ell_C(e) = \ell_{C'}(e)$ for all edges e on P.*

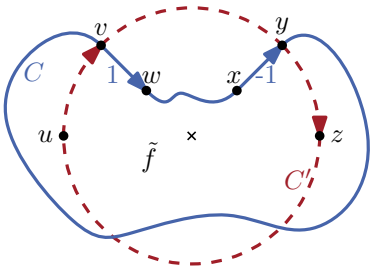

Figure 8 All edges of C' are labeled with 0. In this situation there are edges on C with labels -1 and 1. Hence, C is neither increasing nor decreasing.

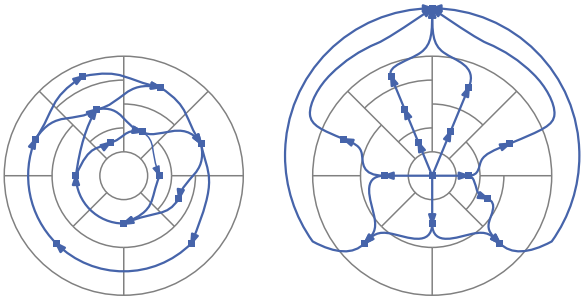

(a) N_{ver} **(b)** N_{rad}

Figure 9 Flow networks N_{ver} and N_{rad} for an example graph G. For simplicity, the edge from the outer to the central face in N_{rad} is omitted.

A monotone essential cycle cannot intersect an essential cycle whose edges are all labeled 0.

▶ **Lemma 4.7.** *Let C and C' be two essential cycles that have at least one common vertex. If all edges on C' are labeled with 0, C is neither increasing nor decreasing.*

Proof Sketch. Consider Fig. 8. Let v be a vertex after which C and C' diverge. Assume C leaves this vertex into the interior (the exterior) of C'. Let y be the vertex where both cycles converge again. Then, C enters y from the interior (the exterior) of C. Thus, one of the edges uw and xy must be labeled positively and the other one negatively. ◀

5 Characterization of Rectangular Graphs

In this section, we prove Theorem 3.5 for rectangular graphs. A *rectangular graph* is a graph together with an ortho-radial representation in which every face is a rectangle, i.e., all incident angles are 90° or 180°. We define two flow networks that assign consistent lengths to the graph's edges, one for the vertical and one for the horizontal edges. These networks are straightforward adaptions of the networks used for drawing rectangular graphs in the plane [7]. In the following, *vertex* and *edge* refer to the vertices and edges of the graph G, whereas *node* and *arc* are used for the flow networks.

The network $N_{\text{ver}} = (F_{\text{ver}}, A_{\text{ver}})$ with nodes F_{ver} and arcs A_{ver} for the vertical edges contains one node for each face of G except for the central and the outer face. All nodes have a demand of 0. For each vertical edge e in G, which we assume to be directed upwards, there is an arc $a_e = fg$ in N_{ver}, where f and g denote the face left and right of e, respectively. The flow on a_e has the lower bound $l(a_e) = 1$ and upper bound $u(a_e) = \infty$. An example of this flow network is shown in Fig. 9a.

To obtain a drawing from a flow in N_{ver}, we set the length of a vertical edge e to the flow on a_e. The conservation of the flow at each node f ensures that the two vertical sides of the face f have the same length.

Similarly, the network N_{rad} assigns lengths to the radial edges. There is a node for each face of G, and an arc $a_e = fg$ for every horizontal edge e in G, which we assume to be oriented clockwise. Additionally, N_{rad} includes one arc from the outer to the central face. Again, all edges require a minimum flow of 1 and have infinite capacity. The demand of all nodes is 0. Fig. 9b shows an example of such a flow network.

▶ **Observation 5.1.** *A pair of valid flows in N_{rad} and N_{ver} bijectively corresponds to a valid ortho-radial drawing of G respecting Γ.*

This immediately follows from the construction of the flow networks.

▶ **Theorem 5.2.** *Let (G, Γ) be a rectangular graph and its ortho-radial representation. If Γ is valid, there exists a bend-free ortho-radial drawing of G respecting Γ.*

Proof Sketch. The fact that such a flow exists in N_{rad} is analogous to the orthogonal case [15]. The key is to show that a valid circulation F_{ver} in N_{ver} exists if Γ is valid. The main idea is to determine for each arc a of N_{ver} a cycle C_a in N_{ver} that contains a. If F_a denotes the circulation that pushes one unit of flow along the arcs of C_a and is 0 elsewhere, then $F_{\text{ver}} = \sum_{a \in A} F_a$, where A denotes the arc set of N_{ver}, is the desired flow. The only reason why such a cycle C_a might not exist is if there is a set S of vertices in N_{ver} such that there exists an arc entering S but no arc exiting S. Without loss of generality, we assume the subnetwork of N_{ver} induced by S to be weakly connected, which implies that S corresponds to a connected set $\mathcal{S}$ of faces in G. Note that S contains a directed cycle of N_{ver}, which is an essential cycle. Let C and C' denote the smallest and largest essential cycle of G, respectively, such that all faces in $\mathcal{S}$ lie in the interior of C and in the exterior of C'. We show that C is increasing or C' is decreasing.

Assume there is an arc a entering S that crosses C (an incoming arc crossing C' is similar). Since all faces are rectangles, there is an elementary path P from $e^\star$ to a vertex v on C using only right and down edges of G. Thus, if w is the first vertex of C after v, it is $\ell_C(vw) = 0$ if vw is horizontal and $\ell_C(vw) = -1$ if vw points up. Since no edge on C is pointing downward, i.e., its label is congruent to $1 \mod 4$, and the labels between adjacent edges differ by $-1, 0$, or 1, it follows that $\ell_C(e') \in \{-2, -1, 0\}$ for all edges e' of C, i.e., $\ell_C(e') \leq 0$. However, the edge e corresponding to the incoming arc a of S is pointing upwards, and therefore $\ell_C(e) = -1$. Hence C is increasing. ◀

Combining this result with Theorem 3.6 results in the characterization of ortho-radial drawings for rectangular graphs.

▶ **Corollary 5.3** (Theorem 3.5 for Rectangular Graphs)**.** *A rectangular 4-plane graph admits a bend-free ortho-radial drawing if and only if its ortho-radial representation is valid.*

6 Characterization of 4-Planar Graphs

In the previous section we proved for rectangular graphs that there is an ortho-radial drawing if and only if the ortho-radial representation is valid. We extend this result to 4-planar graphs by reduction to the rectangular case. In this section we provide a high-level overview of the reduction; a detailed description is found in [1].

In Section 6.1 we present an algorithm that augments G to a rectangular graph. In Section 6.2 we then apply Corollary 5.3 to show the remaining implication of Theorem 3.5.

6.1 Rectangulation Algorithm

Given a graph G and its ortho-radial representation Γ as input, we present a rectangulation algorithm that augments Γ producing a graph G' with ortho-radial representation Γ' such that all faces except the central and outer face of Γ' are rectangles. Moreover, we ensure that the outer and the central face of Γ' make no turns.

Let u be a vertex that has a left turn on a face f and let vw be an edge on f. Let further t be the vertex before u on f. We obtain an *augmentation* Γ^u_{vw} from Γ by splitting the edge vw into two edges vz and zw introducing a new vertex z. Further, we insert the edge

uz in the interior of f such that uz points in the same direction as tu. For an illustration of an augmentation see Fig. 10.

Without loss of generality, we assume the central and outer faces to be rectangular; this can be achieved by inserting 3-cycles into both faces and connecting them to the graph. Every regular face that is not a rectangle has a left turn. We augment that face with an additional edge such that the left turn is resolved and no further left turns are introduced, which guarantees that the procedure of augmenting the graph terminates.

We further argue that we augment the given representation in such a way that it remains valid. Conditions 1 and 2 of Definition 3.4 are easy to preserve if we choose the targets of the augmentation correctly; the proof is analogous to the proof by Tamassia [15]. In particular, the next observation helps us to check for these two conditions.

▶ **Observation 6.1.** *The representation Γ^u_{vw} satisfies Conditions 1 and 2 of Definition 3.4 if and only if* $\mathrm{rot}(f[u, vw]) = 2$.

We further have to check Condition 3, i.e., we need to ensure that we do not introduce monotone cycles when augmenting the graph.

We now describe the approach in more detail. Tamassia [15] shows that if there is a left turn, there also is a left turn on a face f such that the next two turns on f are right turns. We resolve that left turn by augmenting G, which we sketch in the following. Let u be the vertex at which face f takes that left turn. Let t be the vertex before u on f. We differentiate two major cases, namely that tu is either vertical or horizontal.

Case 1, tu is vertical. Let vw be the edge that appears on f after the two right turns following the left turn at u. We show that creating a new vertex z on vw and adding the edge uz (cf. to Fig. 10a for an example) always upholds validity; see Section 6.2 for details.

Case 2, tu is horizontal. This case is more intricate, because we may introduce decreasing or increasing cycles by augmenting the graph. Fig. 10b shows an example, where the graph does not include a decreasing cycle without the edge uz, but inserting uz introduces one. We therefore do not just consider Γ^u_{vw}, but Γ^u_e for a set of *candidate edges* e, which include all edges $v'w'$ on f such that $\mathrm{rot}(f[u, v'w']) = 2$. Hence, Condition 1 and Condition 2 are satisfied by Observation 6.1. If there is a candidate e such that Γ^u_e does not contain a monotone cycle, we are done.

So assume that there is no such candidate and, furthermore, assume without loss of generality that tu points to the right. Let the set of candidates be ordered as they appear on f. We show that introducing an edge from u to the first candidate never introduces an increasing cycle, while introducing an edge from u to the last candidate never introduces a decreasing cycle. This also implies that there must be a consecutive pair of candidates vw and $v'w'$ such that introducing an edge from u to vw creates a decreasing cycle and introducing an edge from u to $v'w'$ creates an increasing cycle.

In Section 6.2 we show that in that case, one of the edges uw or uv' can be inserted without introducing a monotone cycle. Together with Observation 6.1, this proves that we can always remove left turns from the representation while maintaining validity.

Altogether, the algorithm consists of first finding a suitable left turn in the representation, then determining which of the two cases applies and finally performing the augmentation. In particular, when augmenting the graph, we need to ensure that we do not introduce monotone cycles. Checking for monotone cycles can trivially be done by testing all essential cycles. However, this may require an exponential number of tests and it is unknown whether testing the existence of a monotone cycle can be done in polynomial time.

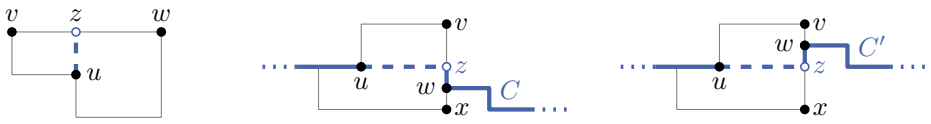

(a) Γ^u_{vw} **(b)** Γ^u_{vw} **(c)** Γ^u_{wx}

Figure 10 Examples of augmentations. (a) Inserting uz is valid, if uz points upwards. (b) The representation Γ^u_{vw} is not valid since inserting the new edge introduces a decreasing cycle C. (c) The candidate wx instead gives the valid representation Γ^u_{wx}. The cycle C', which uses the same edges outside of f as C before, is neither in- nor decreasing.

6.2 Correctness of the Rectangulation Algorithm

Following the proof structure outlined in the previous section we argue more detailedly that a valid augmentation always exists. We start with Case 1, in which the inserted edges is vertical and show that a valid augmentation always exists.

▶ **Lemma 6.2.** *Let vw be the first candidate edge after u. If the edge of f entering u points up or down, Γ^u_{vw} is a valid ortho-radial representation of the augmented graph $G + uz$.*

Proof. Assume that Γ^u_{vw} contains a simple monotone cycle C. As Γ is valid, C must contain the new edge uz in either direction (i.e., uz or zu). Let f' be the new rectangular face of $G + uz$ containing u, v and z, and consider the subgraph $H = C + f'$ of $G + uz$. According to Lemma 4.5 there exists a simple essential cycle C' that does not contain uz. Moreover, C' can be decomposed into paths P and Q such that P lies on f' and Q is a part of C.

The goal is to show that also C' is monotone. We present a proof only for the case of increasing C. The proof for decreasing cycles can be obtained by flipping all inequalities.

For each edge e on Q the labels $\ell_C(e)$ and $\ell_{C'}(e)$ are equal by Lemma 4.4, hence $\ell_{C'}(e) \leq 0$. For an edge $e \in P$, there are two possible cases. The edge e either lies on the side of f' parallel to uz or on one of the two other sides. In the first case, the label of e is equal to the label $\ell_C(uz)$ ($\ell_C(zu)$ if C contains zu instead of uz). In particular the label is negative.

In the second case, we first note that $\ell_{C'}(e)$ is even, since e points left or right. Assume that $\ell_{C'}(e)$ is positive and therefore at least 2. Then, let e' be the first edge on C' after e that points to a different direction. Such an edge exists, since otherwise all edges on C' would have the label 2 and therefore C' would be decreasing contradicting the assumption that Γ is valid. This edge e' lies on Q or is parallel to uz. Hence, the argument above implies that $\ell_{C'}(e') \leq 0$. However, $\ell_{C'}(e')$ differs from $\ell_{C'}(e)$ by at most 1, which requires $\ell_{C'}(e') \geq 1$. Therefore, $\ell_{C'}(e)$ cannot be positive.

We conclude that all edges of C' have a non-positive label. If all labels were 0, C would not be an increasing cycle by Lemma 4.7. Thus, there exists an edge on C' with a negative label and C' is an increasing cycle in Γ. But as Γ is valid, such a cycle does not exist, and therefore C does not exist either. Hence, Γ^u_{vw} is valid. ◀

In Case 2 the inserted edge is horizontal. If there is a candidate e such that Γ^u_e is valid, we choose this augmentation and the left turn at u is removed successfully. Otherwise, we make use of the following structural properties. As before we assume that uz points to the right; the other case can be treated analogously. Using a similar, though technically somewhat more difficult approach as in Lemma 6.2 one can show that augmenting with the first and last candidate does not create increasing and decreasing cycles, respectively.

▶ **Lemma 6.3.** *Let vw be the first candidate after u. No increasing cycle exists in Γ^u_{vw}.*

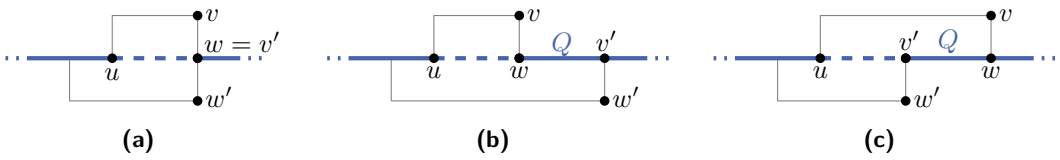

Figure 11 Three possibilities how the path between w and v' can look like: (a) $w = v'$, (b) all edges point right, and (c) all edges point left. In the first two cases the edge uw is inserted and in (c) uv' is added.

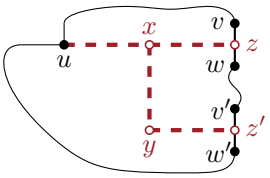

Figure 12 The structure that is used to simulate the insertion of both uz and uz' at the same time. The edge uz is replaced by the path uxz and uz' by $uxyz'$.

▶ **Lemma 6.4.** *Let vw be the last candidate before u. No decreasing cycle exists in Γ^u_{vw}.*

By assumption Γ^u_e contains a monotone cycle for each candidate edge e. From Lemma 6.3 and Lemma 6.4 it follows that there are consecutive candidates vw and $v'w'$ such that Γ^u_{vw} has a decreasing cycle and $\Gamma^u_{v'w'}$ has an increasing cycle.

▶ **Lemma 6.5.** *Let Q be the path on f between the candidates vw and $v'w'$. Then, Q can be completed to a path P in G containing w, v' and u whose edges all point to the right. More precisely, P starts at w or v' and ends at u, and either Q or $\overline{Q}$ forms the first part of P. Moreover, the start vertex of P has no incident edge to its left.*

Proof Sketch. We introduce a construction inside f that simulates the augmentations Γ^u_{vw} and $\Gamma^u_{v'w'}$ at the same time; see Fig. 12. With this construction the resulting representation essentially contains both the increasing cycle of $\Gamma^u_{v'w'}$ and the decreasing cycle of Γ^u_{vw}. Using this, we show that both cycles use Q and thus Q must only point to the right. Similarly, we show that both cycles are equal outside of f, which implies that all corresponding edges also point to the right. Hereby, these edges together with Q form the desired path P. ◀

There are three possible ways how the vertices w and v' can be arranged on P; see Fig. 11. Either $w = v'$, w comes before v', or v' comes before w. In any case we denote the start vertex of P by z. According to Lemma 6.5, no edge is incident to the left of z. Hence, the insertion of the edge uz such that it points right gives a new ortho-radial representation Γ', which is valid by the following lemma.

▶ **Lemma 6.6.** *Let Γ' be the ortho-radial representation that is obtained from Γ by adding the edge uz pointing to the right as in Lemma 6.5. Then, Γ' is valid.*

Proof. By construction, Γ' satisfies Conditions 1 and 2 of Definition 3.4. Let $C' = P + uz$ be the new cycle whose edges point right. It is $\ell_{C'}(e) = 0$ for each edge e of C'. Essential cycles without uz or zu are not monotone, since they are already present in the valid representation Γ. If an essential cycle C contains uz or zu and thus the vertex u, Lemma 4.7 states that C is not monotone. Thus, Γ' satisfies Condition 3 and is therefore valid. ◀

Putting all results together we see that the rectangulation algorithm presented in Section 6.1 works correctly. That is, given a valid ortho-radial representation Γ, the algorithm produces another valid ortho-radial representation Γ' such that all faces of Γ' are rectangles and Γ is contained in Γ'. Combining this result with Theorem 5.2 we obtain the following theorem.

▶ **Theorem 6.7.** *Let Γ be a valid ortho-radial representation of a graph G. Then there is a drawing of G representing Γ.*

This shows the remaining implication of Theorem 3.5 thus completing the characterization.

7 Conclusion

In this paper we considered orthogonal drawings of graphs on cylinders. Our main result is a characterization of the 4-plane graphs with a fixed embedding that can be drawn bend-free on a cylinder in terms of a combinatorial description of such drawings. These ortho-radial representations determine all angles in the drawing without fixing any lengths, and thus are a natural extension of Tamassia's orthogonal representations. However, compared to those, the proof that every valid ortho-radial representation has a corresponding drawing is significantly more involved. The reason for this is the more global nature of the additional property required to deal with the cyclic dimension of the cylinder.

Our ortho-radial representations establish the existence of an ortho-radial TSM framework in the sense that they are a combinatiorial description of the graph serving as interface between the "Shape" and "Metrics" step.

For rectangular 4-plane graphs, we gave an algorithm producing a drawing from a valid ortho-radial representation. Our proof reducing the drawing of general 4-plane graphs with a valid ortho-radial representation to the case of rectangular 4-plane graphs is constructive; however, it requires checking for the violation of our additional consistency criterion. It is an open question whether this condition can be checked in polynomial time. These algorithms correspond to the "Metrics" step in a TSM framework for ortho-radial drawings.

Since the additional property of the characterization is non-local (it is based on paths through the whole graph), the original flow network by Tamassia cannot be easily adapted to compute a bend-minimal valid ortho-radial representation, which would correspond to the "Shape" step of an ortho-radial TSM framework. We leave this as an open question.

References

1 Lukas Barth, Benjamin Niedermann, Ignaz Rutter, and Matthias Wolf. Towards a topology-shape-metrics framework for ortho-radial drawings. *CoRR*, arXiv:1703.06040, 2017.

2 Therese Biedl and Goos Kant. A better heuristic for orthogonal graph drawings. *Computational Geometry: Theory and Applications*, 9:159–180, 1998.

3 Thomas Bläsius, Marcus Krug, Ignaz Rutter, and Dorothea Wagner. Orthogonal graph drawing with flexibility constraints. *Algorithmica*, 68(4):859–885, 2014.

4 Thomas Bläsius, Sebastian Lehmann, and Ignaz Rutter. Orthogonal graph drawing with inflexible edges. *Computational Geometry: Theory and Applications*, 55:26–40, 2016.

5 Thomas Bläsius, Ignaz Rutter, and Dorothea Wagner. Optimal orthogonal graph drawing with convex bend costs. *ACM Transactions on Algorithms*, 12:33:1–33:32, 2016.

6 Sabine Cornelsen and Andreas Karrenbauer. Accelerated bend minimization. *Journal of Graph Algorithms and Applications*, 16(3):635–650, 2012.

7 Giuseppe Di Battista, Peter Eades, Roberto Tamassia, and Ioannis G. Tollis. *Graph Drawing – Algorithms for the Visualization of Graphs*. Prentice Hall, 1999.

8 Giuseppe Di Battista, Giuseppe Liotta, and Francesco Vargiu. Spirality and optimal orthogonal drawings. *SIAM Journal on Computing*, 27(6):1764–1811, 1998. doi:10.1137/S0097539794262847.

9 Christian A. Duncan and Michael T. Goodrich. *Handbook of Graph Drawing and Visualization*, chapter Planar Orthogonal and Polyline Drawing Algorithms, pages 223–246. CRC Press, 2013.

10 Ashim Garg and Roberto Tamassia. On the computational complexity of upward and rectilinear planarity testing. *SIAM Journal on Computing*, 31(2):601–625, 2001.

11 Madieh Hasheminezhad, S. Mehdi Hashemi, Brendan D. McKay, and Maryam Tahmasbi. Rectangular-radial drawings of cubic plane graphs. *Computational Geometry: Theory and Applications*, 43:767–780, 2010.

12 Mahdie Hasheminezhad, S. Mehdi Hashemi, and Maryam Tahmabasi. Ortho-radial drawings of graphs. *Australasian Journal of Combinatorics*, 44:171–182, 2009.

13 Md. Saidur Rahman, Shin-ichi Nakano, and Takao Nishizeki. Rectangular grid drawings of plane graphs. *Computational Geometry: Theory and Applications*, 10:203–220, 1998.

14 Md. Saidur Rahman, Takao Nishizeki, and Mahmuda Naznin. Orthogonal drawings of plane graphs without bends. *Journal of Graph Algorithms and Applications*, 7(3):335–362, 2003.

15 Roberto Tamassia. On embedding a graph in the grid with the minimum number of bends. *SIAM Journal on Computing*, 16(3):421–444, 1987.